ESR dating of quartz grains: evaluating the performance of various cryogenic systems for dosimetric purpose

Verónica Guilarte [1*], Fang Fang [2], Rainer Grün [2], Mathieu Duval [3,4]

[1]Departament of Didáctica de las Ciencias Experimentales, Facultad de Ciencias de la Educación y del Deporte de Melilla. Universidad of Granada, Spain

[2] Research School of Earth Sciences, Australian National University, Canberra ACT 2601, Australia

[3] Centro Nacional de Investigación sobre la Evolución Humana (CENIEH), Burgos, Spain

[4] Australian Research Centre for Human Evolution (ARCHE), Environmental futures Research Institute, Griffith University, Nathan QLD 4111, Australia

*Corresponding author: veronicaguilarte@ugr.es

Abstract

We present the results of the first detailed comparative and quantitative study of various cryogenic systems that can be used for ESR measurements of quartz grains. Three experimental setups were tested: (i) a standard liquid nitrogen Variable Temperature Unit (VTU), operating at 90-100 K and used in most ESR dating studies; (ii) a helium-based VTU that can reach measurement temperatures as low as 15-20 K; and a (iii) finger dewar filled with liquid nitrogen operating at 77 K.

As expected, our results show significant gains in signal intensity and resolution when working at temperatures below 90 K, which is extremely useful when dealing with samples with weak intensities or poorly-resolved spectra. The improved signal resolution at 40 K allows the differentiation of the Ti-Li and Ti-H absorption lines around g = 1.913 that are typically merged at 90 K or above. It is therefore possible to extract the ESR intensity of a resolved Ti-Li signal for dating.

The results obtained with each experimental configuration are highly consistent for both the Al and Ti centres. Eleven of twelve samples agree at a 1σ level, and no significant systematic bias was observed between the cryogenic systems.

Keywords: Electron Spin Resonance dating; quartz grains; dosimetry; cryogenic temperatures; Finger Dewar.

Introduction

Electron Spin Resonance (ESR) dating of quartz grains is based on the detection of radiation-induced paramagnetic centres in quartz (Weil, 1984; Toyoda et al., 2015). The aluminium $[AlO_4]^0$ and titanium centres $[TiO_4/M^+]^0$ (M^+= Li^+ and H^+) have become widely used for dating since the first application by Yokoyama et al. (1985). However, unlike the ESR signals in other materials, such as fossil tooth enamel, corals or carbonates, the Al and Ti centres in quartz are not visible at room temperature, and measurements must be performed at low (cryogenic) temperatures (<120 K; e.g. Guilarte and Duval, 2020).

Most ESR dating laboratories use liquid nitrogen (N_2) variable temperature units (VTU), with a temperature range of between 85 to 120 K, and to a lesser extent a finger dewar filled with liquid N_2, reaching 77 K (see Table 1 from Guilarte and Duval, 2020). Other experimental setups, e.g, liquid Helium (He) VTU can reach lower temperatures, but have never been used for dating, to our knowledge.

While measurement temperature is known to have a direct impact on both, the intensity and the spectral resolution of the ESR signals of the Al and Ti centres (e.g. Duval and Guilarte, 2012; Shimada and Toyoda, 2004), its influence on equivalent dose (D_E) determinations has rarely been studied. Duval and Guilarte (2012) ran initial comparison tests at 120 K, 110 K and 90 K, the most common measurement temperature range employed in the community, and observed no significant differences in the D_E values for a couple of quartz samples. Only a few laboratories have been working at lower temperature using a finger dewar (77 K) (e.g., Burdette et al., 2012; Liu et al., 2010; Ji et al., 2021; Wei et al., 2020), while we have no record of any ESR dating work using temperatures below 77 K. As in luminescence dating, methodological studies are required to establish the basis for the standardisation of analytical procedures in ESR dating of quartz grains. In that regard, the present work is a follow up on the previous study by Guilarte and Duval (2020), who demonstrated that the use of different ESR spectrometers and resonators do not significantly bias the dose evaluation. Here, we study the influence of temperature on ESR intensity and spectral resolution from 20 to 100 K, and especially, the potential and drawbacks of the different cryogenic setups used in ESR spectroscopy. We specifically evaluate the

performance of three different temperature systems: (i) an evaporative liquid N_2 VTU (measurement temperature ~ 90-100 K), (ii) a liquid He VTU (operating between 20 and 100K), (iii) a finger dewar, in which sample tubes are directly inserted into liquid N_2 (measurement temperature = 77 K). This is the first time to our knowledge that such a quantitative comparison study has been carried out.

1. Materials and Methods

1.1 Sampling and sample preparation

Six quartz samples (100-200 µm) were selected for the experiments. PAN1201, PAN1202 and PAN1203 come from the Early Pleistocene palaeontological locality of Pantalla, Italy (e.g., Cherin et al., 2014), while OUR1101 was collected from the Middle Pleistocene site of Oued Rabt, Morocco (Sala et al., 2020). Samples BUR1107 was taken from the palaeontological locality of Villarroya (Pueyo et al., 2016) and BUR1118 from the Middle Pleistocene fluvial deposits of the Tirón river (Spain). All samples were prepared following the standard procedures of the ESR dating laboratory at CENIEH (e.g., Duval et al., 2017).

The extracted quartz of each sample was divided into 12-14 multiple grain aliquots. 10 to 12 of these aliquots were irradiated with a ^{60}Co or a ^{137}Cs gamma source using increasing irradiation doses. The non-bleachable residual ESR signal intensity of the Al centre was evaluated by exposing one aliquot of each natural sample in a SOL2 (Dr Hönle) solar light simulator for more than 1000 h. One aliquot of each sample was kept unirradiated and unbleached (= natural aliquot). Sample preparation and gamma irradiation procedures are described in more detail in the Supplementary Information section.

1.2 ESR measurements

1.2.1 Experimental setups

The experiments were carried out in the ESR dating laboratory at CENIEH (Spain) with two different cryogenic systems (N_2 VTU and He VTU) and in the Centre for Advanced Imaging (CAI) at the University of Queensland, Australia (finger dewar), see Table 1. The following three setups were used:

- A liquid N_2 VTU, see Barr (1999). Although the minimum temperature certified by the manufacturer is 100 K, Duval and Guilarte Moreno (2012) showed that the CENIEH system can reach a minimum temperature of 85 K, and stable temperatures (± 0.1 - 0.2 K) can be achieved for several hours at 90 K.

- A He VTU, allowing measurements at temperatures as low as ~15-20 K. Here, we used 90 K and 35-40 K for dose evaluation.
- A finger dewar, filled with liquid nitrogen. While this does not allow temperature adjustments, it ensures a completely stable measurement temperature at 77 K.

1.2.2 Acquisition parameters

The Al and Ti centres were measured in the three experimental setups using acquisition parameters as similar as possible (Table 2). The receiver gain was optimized with the highest irradiated aliquot of each sample. The other acquisition parameters correspond to N_2 VTU, which is routinely used at CENIEH (e.g., Duval et al., 2017). These were initially optimized following international standards for ESR retrospective dosimetry (e.g., ISO/DIS 13304) and other reference books (e.g., Höfer, 2009; Eaton et al., 2010).

When using the finger dewar, air bubbles can randomly appear during the ESR measurement, making the resulting spectrum unusable. This can be addressed by reducing the sweep time and increasing the number of successively acquired scans. Thus, the conversion time was set to 20 ms, reducing the sweep time for each scan from 40.96 s and 61.44 s with the VTU setups to 20.48 s for the Al and Ti signals, respectively (Table 2). The number of scans ranged from 4 to 12, depending on signal intensity. All acquisition parameters are listed in Table 2.

1.2.3 Measurement conditions and D_E evaluation

To ensure similar resonance conditions, all the aliquots of a given sample were weighed in separate quartz tubes with a precision of < 0.5% (1 mg). The precision of the measurements was optimized by carefully aligning the centre of the sample in the quartz tube with the centre of the cavity (Guilarte and Duval, 2020).

Dose Response Curves (DRC) for each sample were obtained using the Multiple Aliquots Additive (MAA) dose method. BUR1107 and BUR1118 were measured with the N_2 VTU and the He VTU (at 90 K and 35-40 K), while the N_2 VTU and the finger dewar were used for the four samples from Pantalla and Oued Rabt. When possible, each aliquot was measured 3 times after ~120 º rotation in the resonator to account for angular heterogeneity. Each sample was repeatedly measured up to three times over different days (Supplementary Information Table S2, S3 and S4).

The intensity of the Al centre was the difference between the top of the first peak (g = 2.0185) and the bottom of the 16th peak (g = 1.9928, see Figure 1) (Toyoda and Falguères, 2003). The intensities of the Ti centre (Ti-Li + Ti-H) were evaluated by measuring the peak-

to-baseline amplitude around g = 1.915 – 1.913 (option D, Figure 1) and peak-to-peak amplitude between g = 1.979 and 1.915-1.913 (option A of Duval and Guilarte, 2015) (Figure 1). Using the He VTU 35-40 K, the improved spectral resolution at 40 K made it possible to isolate the Ti-Li peak around g = 1.913 and extract the corresponding intensity (see Figure 1). ESR intensities were corrected for receiver gain, number of scans and mass. The details of DRC fitting (software, fitting functions, data weighting) are given in the Supplementary Information section.

2. Results and discussion

2.1.ESR signal intensity and spectral resolution

The He VTU allows the study of the signal behaviour at temperature as low as 20 K. For dosimetric purposes, temperature and microwave power must be optimized in order to maximize signal intensity and spectral resolution. As microwave saturation depends on the measurement temperature (Shimada and Toyoda, 2004), various tests using microwave powers (from 0.1 mW to 10 mW) at different temperatures were carried out. Figure 2 shows the microwave saturation curves obtained for temperatures ranging from 20 to 80 K for both Al and Ti (option D) signals. Signal intensity saturation was observed at low microwave power (< 1 mW) for temperatures < 30 K. A microwave power of 2 mW was considered as optimal for temperatures of 35 K (Al centre) and 40 K (Ti centre), and was therefore used in the comparison of the three cryogenic systems (see Table 2).

Sample BUR1107 was measured from 20 to 110 K (one scan each, see Figure 3) in 5 K steps. Resolution and signal intensity of the ESR spectra are clearly temperature dependent and are maximised at around 30 to 40 K (see Figure 3). The most striking effect is the improved resolution of two peaks around g = 1.913 for the Ti (Ti-Li and Ti-H) centres, which are usually merged into one single peak at temperatures > 77 K (see also Supplementary Information Figure S1). Thus, measurements at 40 K enables the extraction of the non-interferred Ti-Li signal for dating.

The temperature responses of the Al and Ti (option D) centres were fitted with 6th order polynomial functions. It can be seen in Figure 3 that the temperature dependence of the Al and Ti (option D) centres is different. The peak to peak Al centre signal intensity is 3.4 times higher at 35 K than at 90 K (same temperature as N_2 VTU setup), and almost 2 times higher than at 77 K (same temperature as finger dewar setup). In comparison, the intensity of the Ti (option D) centre shows less increase: it is 1.8 and 1.3 higher than at 90 K and 77 K, respectively. Ti

(option A) behaves similarly, being also 1.8 and 1.3 times higher at 40 K than at 77 K and 90 K, respectively. Finally, below 30 K, the ESR signals of the Al and Ti centres become saturated at 2 mW microwave power and the intensities dramatically decrease (see also Figure 2 and Shimada and Toyoda, 2004). Signal saturation at low temperature is due to the spin-lattice relaxation (T1): this process is not very effective at very low temperature, and as a consequence, the spin-lattice relaxation time increases, and the absorption signal is readily saturated (Bertrand, 2010). However, when temperature increases, relaxation processes become efficient and lead to rapid shortening of T1. This shortening induces a broadening of the spectral lines, as shown in Al and Ti centres spectra.

Various quartz samples of distinct origin were measured to check whether the temperature behaviour of the Al and Ti centres is sample dependent (Figure 4**)**. For all samples, the Al signal intensity increases by about 4 times from 90 K to 35 K, and about 1.8 times for the Ti (option D) centre. The slight differences observed among samples are not statistically significant.

Figure 2 shows that good signal intensities can already be achieved at 60 K using a microwave power of 5 mW or around 77 K with a microwave power of 10 mW. However, 35-40 K was chosen due to the improved spectral resolution for both the Al and Ti centres, and to evaluate the full potential of the Helium system for ESR dosimetry.

2.2. Dose Response Curves

The Al and Ti centre DRCs of the 6 samples were measured with the different experimental setups and following the conditions detailed in Materials and Methods. For comparison, BUR 1107 and BUR1118 were measured with the N_2 VTU and the He VTU (90 K and 35-40 K), and the four samples from Pantalla and Oued Rabt using the N_2 VTU and the finger dewar.

The detailed fitting results of the DRCs are provided in Supplementary Information Tables S2 to S4, while all DCRs are shown in Figures S2 to S7. To ease comparison, normalised DRCs are shown in Figures S8 and S9.

Measurements over successive days may give insights into the stability of the N_2 VTU and the finger dewar (Supplementary Information Table S3 and S4). We did not carry out such measurements for the He VTU. The overall measurement precision using the N_2 VTU ranged between 2.3-2.6 % (Al centre) and 2.5-3.5 % (Ti centre, options A and D); and for the finger dewar between 1.8-2.3 % (Al) and 2.8-5.3 % (Ti). The finger dewar showed a slightly better precision for the Al signal intensities (by 0.2-0.7 %) compared to the N_2 VTU, while for all but one sample, the Ti (options A and D) signal showed the opposite behaviour

193 and with a larger difference (0.7-2.3%). The higher scatter of the Ti data compared with the
194 Al intensities lies in the relative signal-to-noise ratios, which are much lower for the Ti centre
195 (Duval and Guilarte, 2015).

196 The normalised DRCs for the Al centre (Figures S8 and S9) show that the intensities of
197 the He and N_2 VTUs are either close (BUR1107) or randomly scattered (BUR1118). The N_2
198 VTU and the finger dewar provide comparable intensities at doses < 10000 Gy, while the
199 finger dewar (77 K) yields slightly smaller ESR intensities at higher doses compared with
200 the N_2 VTU (90 K) for 3/4 of the samples. For the Ti centre (options A and D), most samples
201 show an opposite behaviour except for sample OUR1101. The normalised ESR intensities
202 are higher with the decreasing of temperatures (BUR1107, BUR1118, PAN1201, PAN1202,
203 PAN1203). This may be partly related to the higher spectral resolution obtained at lower
204 temperature, which enables a better separation of the Ti-Li and Ti-H absorption lines. In
205 other words, at temperature < 90 K, the ESR intensity of the peak around g = 1.913 (Option
206 D of Duval and Guilarte, 2015) has a higher relative contribution from the Ti-Li centre which
207 is known to reach saturation at higher doses (Duval and Guilarte, 2015). This hypothesis is
208 supported by the "pure" Ti-Li DRCs that can be obtained at 40 K for samples BUR1107 and
209 BUR1118 (Figure S8), which show much higher intensities than those from option D.

210 ***2.3.D_E values***

211 Figure 5 and Table S2 summarise all D_E results. The Al centre in BUR1107 and BUR1118
212 yielded consistent D_E values for the different experimental setups (N_2 VTU and He VTU at
213 90 K and 35-40 K). The DRCs of these samples could be well fitted, all r^2 values were >
214 0.97 (see Table S2). The same applied to the Ti (option A and D) and Ti-Li centres, with
215 consistent D_E values and r^2 values of > 0.96, and most of them > 0.99.

216 The Al centre of the other samples yielded consistent D_E values at either 1σ (Pantalla
217 samples) or 2σ (OUR1101) for the N_2 VTU and the finger dewar applying a double
218 saturating exponential (DSE) fitting function (Figure 5**,** Tables S3 and S4). Fitting the data
219 points with a DSE as well as with an exponential plus a linear function (Exp+lin) show good
220 results (r^2 ~ 0.99) for both setups, the DSE having slightly higher r^2 values (Figures S4a,
221 S4b and S6). Thus, the D_E values in Figure 5 were derived from fitting with a DSE.

222 The dose response of the signal intensities derived from the Ti centres (option A and D)
223 were fitted with a Ti-2 function (equation 1) as well as with a single saturating exponential
224 (SSE) function (see details about the fitting functions in Table S1). Good results were
225 obtained with both functions and all r^2 values > 0.94. However, the Ti-2 function gave

slightly better results for almost all DRCs. Ti centre (option A) provided consistent results for the D_E values using the N_2 VTU and the finger dewar for all Pantalla and Oued Rabt samples, except for PAN1202. All D_E values derived from the Ti centre (option D) are consistent within statistical error for both setups (Tables S3 and S4).

$$I = a * \left(\left(e^{-\left(\frac{D+D_E}{D_1}\right)} \right) - \left(e^{-\left(\frac{D+D_E}{D_2}\right)} \right) \right) \qquad \text{(Equation 1)}$$

All D_E values agree within 1-σ for both the Al and Ti (option D) centres except for the Al centre in OUR1101. There is no apparent systematic bias between the setups. The results demonstrate that in spite of some differences in the ESR intensities (section 2.2.), the three experimental setups yield consistent dose estimates and can be independently used for ESR dating purposes. In addition, the different measurement temperatures employed (90 K, 77 K and 35-40 K) yielded consistent D_E values, as was previously observed by Duval and Guilarte Moreno (2012) who performed measurements at 90 K, 100 K and 110 K. In summary, our results obtained from a wide temperature range from 110 K to 35 K indicate that there is no noticeable impact of temperature on the dose results.

Comparing the potential of the three different setups, the N_2 VTU, with measurement temperatures between 90 and 100 K, can provide reliable results for most of the quartz samples showing sufficient signal intensity. In comparison, the much cheaper finger dewar reaches lower temperatures (77 K), yielding a significant gain in the signal-to-noise ratio and resolution if required. Although the results suggest that this increase in signal intensity could reduce the acquisition time, in practice, the interference created by the random appearance of air bubbles may complicate these measurements for the Ti centre. Interferences caused by bubbles could be reduced by adding a metal coil outside the sample tube. For Al centre measurements, signal to noise ratio (S/N) is > 70 and multiple scans are not needed. However, for Ti centre, the acquisition of several scans is required to achieve a spectrum with sufficient S/N ratio, increasing the risk for bubbles to appear during the measurements. As a result, comparable acquisition times may be needed with the finger dewar. On the other hand, significantly less liquid nitrogen is required for the finger dewar measurements compared to the N_2 VTU at 90 K (by a factor of 5), reducing the cost associated with this cryogenic liquid. The He-based VTU offers significant advantages with respect to signal resolution and intensity, including the identification of the Ti-Li absorption line at g=1.913. This could be interesting for further studies into the nature and behaviour of complex signals, which could lead to more accurate dose assessment procedures. However, the higher cost of the liquid helium and the much more

complex equipment associated with the He VTU would significantly increase the costs for ESR dating. For routine, low temperature ESR measurements, either the N_2 VTU or the finger dewar offer the best balance between measurement time/stability, signal resolution/intensity, and measurement cost.

Conclusions

After Duval and Guilarte Moreno (2012) and Guilarte and Duval (2020), this is the third work of a long-running methodological investigation aiming at thoroughly evaluate (i) the overall influence of temperature on ESR measurements of quartz grains, with a special focus on signal intensity and resolution as well as on dose determination, and (ii) the bias potentially induced by the equipment employed, particularly the spectrometer, cavity and cryogenic systems. While the initial study by Duval and Guilarte Moreno (2012) evaluated the performance and stability of the Bruker EMXmicro spectrometer coupled with a liquid nitrogen VTU for long acquisitions at low temperature, Guilarte and Duval (2020) demonstrated later that the use of different ESR spectrometers and resonators do not induce any significant bias in the dose evaluation. The present study shows that liquid helium- and nitrogen-based VTUs as well as finger dewars yield consistent dose estimates.

It is actually reassuring that all combinations of cryogenic systems, spectrometers and resonators provide closely similar dose estimates. It allows the comparison of results among laboratories using different ESR equipment, which could contribute to develop standardised measurement procedures for ESR dating at low temperature.

Acknowledgements

MD would like to thank Lee J. Arnold (University of Adelaide), Alfonso Benito Calvo (CENIEH), Marco Cherin (University of Perugia), Josep M. Parés (CENIEH) and Arsenio Muñoz (University of Zaragoza) for their help with the ESR sampling at Pantalla, Oued Rabt and Villarroya localities. The analytical costs associated to the ESR dating of some of these samples were covered by Spanish grants CGL 2010-16821 (Spanish Ministry of Science and Innovation) and CEN001B10-2 (Junta de Castilla y León, Consejería de Educación). Aspects of this work were funded by the Spanish Ramón y Cajal Fellowship RYC2018-025221-I granted to M.D. The authors would like to thank Jeffrey Harmer, UQ, for giving access to the CAI facilities and for his support during measurements.

References

Barr, D. (1999). EMX User's Guide for the ER 4131VT Variable Temperature Accessory. Manual Version 1.0. Bruker Instruments, Inc.

Bertrand, P. (2020). Electron Paramagnetic Resonance Spectroscopy. Fundamentals. Springer, Nature Switzerland.

Burdette, K.E., Rink, W.J., Mallinson, D.J., Means, G.H., Parham, P.R., 2013. Electron spin resonance optical dating of marine, estuarine, and aeolian sediments in Florida, USA. Quat. Res. 79(1): 66-74. https://doi.org/10.1016/j.yqres.2012.10.001

Cherin, M., Iurino, D.A., Sardella, R. Rook, L., 2014. Acinonyx pardinensis (Carnivora, Felidae) from the Early Pleistocene of Pantalla (Italy): predatory behavior and ecological role of the giant Plio–Pleistocene cheetah. Quat. Sci. Rev. 87, 82-97. https://doi.org/10.1016/j.quascirev.2014.01.004

Duval, M., Guilarte Moreno, V., 2012. Assessing the influence of the cavity temperature on the ESR signal of the Aluminum center in quartz grains extracted from sediment. Ancient TL 30 (2), 51-56.

Duval, M., Guilarte, V., 2015. ESR dosimetry of optically bleached quartz grains extracted from Plio-Quaternary sediment: Evaluating some key aspects of the ESR signals associated to the Ti-centres. Radiat. Meas. 78, 28-41. https://doi.org/10.1016/j.radmeas.2014.10.002

Duval, M., Arnold, L.J., Guilarte, V., Demuro, M, Santonja, M., Pérez-González, A., 2017. Electron Spin Resonance dating of optically bleached quartz grains from the Middle Palaeolithic site of Cuesta de la Bajada (Spain) using the multiple centres approach. Quat. Geochronol. 37, 82-96. https://doi.org/10.1016/j.quageo.2016.09.006

Eaton, G.R., Eaton, S.S., Barr, D.P., Weber, R.T., 2010. Quantitative EPR. Springer, Wien-New York, p. 185.

Guilarte V., Duval M., 2020. ESR dating of optically bleached quartz grains: intra-laboratory comparison of different experimental setups and their impact on dose evaluation. Geochronometria. https://doi.org/10.2478/geochr-2020-0005

Höfer P, 2009. Basic Experimental Methods in Continuous Wave Electron Paramagnetic Resonance, in: Brustolon, M., Giamello, E. (Eds.), Electron Paramagnetic Resonance: a practitioners toolkit. John Wiley & Sons, Inc., Hoboken, NJ, USA, pp. 37-82.

ISO/DIS 13304, 2011. Radiological protection-Minimun criteria for electron paramagnetic resonance (EPR) spectroscopy for retrospective dosimetry of ionizing radiation. ISO, Geneve.

Ji, H., Liu, C.-R., Yin, G., Wei, C., Song, W., 2021. ESR dating of the Hougou Paleolithic site in the Nihewan Basin, North China, using both additive and regenerative dose methods. Quat. Int. 10.1016/j.quaint.2021.10.001.

Liu, C.R., Yin, G.M., Gao, L., Bahain, J.J., Li, J.P., Lin, M., Chen, S.M., 2010. ESR dating of Pleistocene archaeological localities of the Nihewan Basin, North China – Preliminary results. Quat. Geochronol. 5(2–3): 385-390. https://doi.org/10.1016/j.quageo.2009.05.006

Pueyo, E.L., Muñoz, A., Laplana, C., Parés, J.M., 2016. The Last Appearance Datum of Hipparion in Western Europe: magnetostratigraphy along the Pliocene–Pleistocene boundary in the Villarroya Basin (Northern Spain). Int. J. Earth Sci. (Geol Rundsch). https://doi.org/10.1007/s00531-015-1281-0

Sala-Ramos et al., 2022. Le peuplement humain pendant le Pléistocène et l'Holocène dans la Province de Jerada, Maroc Oriental. Bulletin d'Archéologie Marocaine 27, pp. 27-40.

Shimada, A., Toyoda, S., 2004. The optimal conditions of microwave and temperature of ESR measurement suitable for impurities centers in quartz. Adv. ESR Appl. 21, 13-16.

Toyoda, S., Falguères, C., 2003. The method to represent the ESR signal intensity of the aluminium hole centre in quartz for the purpose of dating. Adv. ESR Appl. 20, 7-10.

Toyoda, S., 2015. Paramagnetic lattice defects in quartz for applications to ESR dating. Quat. Geochronol. 30, 498-505. https://doi.org/10.1016/j.quageo.2015.05.010

Wei, C., Yin, G., Li, Y., Liu, C.-R., Li, W., Guo, R., 2020. Quartz electron spin resonance signal intensity of Al and Ti–Li centers as a provenance indicator: An example from the Yangtze River Basin. Quat. Int. 562, 76-84. https://doi.org/10.1016/j.quaint.2020.06.023 Weil, J.A., 1984. A review of electron-spin spectroscopy and its application to the study of paramagnetic defects in crystalline quartz. Phys. Chem. Minerals 10, 149-165. https://doi.org/10.1007/BF00311472

Yokoyama, Y., Falguères, C., Quaegebeur, J.P., 1985. ESR dating of quartz from quaternary sediments: First attempt. Nucl. Tracks, 10 (4-6), 921-928. https://doi.org/10.1016/0735-245X(85)90109-7

Figure captions

Figure 1. Examples of ESR spectra measured on the natural aliquot of quartz sample BUR1107. Left: ESR signal of Al centre measured at 35and 90 K. The ESR intensity is evaluated as indicated by the vertical solid line. Right: ESR signal of Ti centres measured at 40 K and 90 K for comparison. ESR intensities of the Ti (option D) and Ti (option A) are evaluated as indicated by the vertical solid lines. At 40 K, there is enough resolution to isolate the Ti-Li centre and extract the corresponding intensity by measuring the peak-to-baseline amplitude around g = 1.913.

Figure 2. Saturation intensity curves obtained from sample BUR1107 for Al and Ti (option D) signals. Note that the intensity of the ESR signal increases with the square root of the microwave power in a linear way in the absence of saturation effects (dashed lines). The maximum microwave power that can be used to avoid signal saturation can be determined from the moment this linearity is lost.

Figure 3. Influence of temperature on the ESR signal of Al and Ti (option D) centres (sample BUR1107). Acquisitions were performed with the He VTU. Top graphs: evolution of the ESR signal from T = 35 to 110 K (Al) and from T = 40 to 110 K (Ti). Acquisition parameters: 2 mW microwave power, 1024 points resolution, 100 KHz modulation frequency, 0.1 mT modulation amplitude, 40 ms conversion time for Al and 60 ms for Ti signals, and 1 scan. Bottom graphs: evolution of the ESR intensities (normalized for T = 90 K) with temperature ranging from 20 K to 110 K.

Figure 4. Illustration of the inter-sample variability of the ESR intensity vs. temperature. Left: Al centre measured at 35, 65 and 90 K. Right: Ti (option D) centre measured at 40, 65 and 90 K. To facilitate comparison, all ESR intensities of the different samples have been normalised by their corresponding value at 90 K. Samples BUR1107, BUR1108, BUR1111 come from Villarroya locality (Rioja), TE1002 from Atapuerca (Burgos), BUR1120 from the southern margin of the Duero Basin (Segovia).

Figure 5. Comparison of D_E values obtained from the Al centre and Ti centre measured in various samples with different experimental setups. Errors are 1σ. Corresponding numerical values are given in Supplementary information Tables S2 to S4. For the Al centre, D_E values were obtained by fitting an EXP+LIN function (BUR1107 and BUR1118) or a DSE function (Pantalla and Oued Rabt samples**)**. For the Ti centre (option D and Ti-Li), D_E values were obtained by fitting a SSE (BUR1107 and BUR1118) or a Ti-2 function (Pantalla and Oued

379 Rabt samples**)**. Final DRCs were obtained by using the pool ESR intensities derived from the
380 repeated measurements.

381

382 **Table caption**

383 Table 1. Description of each experimental setup employed in the present work. Key: VTU =
384 Variable Temperature Unit; (1) Measurement temperature range potentially covered by the
385 experimental setup (based on manufacturer's data); (2) Measurement temperature used in the
386 present study.

387 Table 2. Acquisition parameters used in the present study.

388

389 **Table 1.**

	Experimental Setup #1 N_2 VTU	**Experimental Setup #2a He VTU**	**Experimental Setup #2b He VTU**	**Experimental Setup #3 Finger Dewar**
Laboratory	ESR dating laboratory, CENIEH, Spain	ESR dating laboratory, CENIEH, Spain	ESR dating laboratory, CENIEH, Spain	CAI, University of Queensland, Australia
Cryogenic temperature system	VTU ER4141VT Digital Temperature control system	VTU ER4112HV Digital Temperature control system	VTU ER4112 HV Digital Temperature control system	Finger Dewar
Cryogenic liquid	Liquid Nitrogen	Liquid Helium	Liquid Helium	Liquid Nitrogen
Temperature range [(1)]	90-300 K	20-300 K	20-300 K	77 K
Measurement Temperature (DRC)[(2)]	90 K	90 K	35 K (Al) 40 K (Ti)	77 K
ESR spectrometer	Bruker EMX 6/1 micro	Bruker Elexsys E500	Bruker Elexsys E500	Bruker Elexsys E500
Resonator model	ER4102ST: standard cavity	SHQE: high sensitivity cavity	SHQE: high sensitivity cavity	ER4102ST: standard cavity
Acquisition software	Bruker WinEPR	Bruker Xepr	Bruker Xepr	Bruker Xepr

390

391

392 **Table 2.**

	Al centre			Ti centre		
Experimental Setup	**Setup #1 N_2 VTU**	**Setup #2 (a/b) He VTU**	**Setup #3 Finger Dewar**	**Setup #1 N_2 VTU**	**Setup #2 (a/b) He VTU**	**Setup #3 Finger Dewar**
Temperature (K)	90	90 (setup #2a) 35 (setup #2b)	77	90	90 (setup #2a) 40 (setup #2b)	77
Microwave power (mW)	10	2	10	5	2	5
Sweep width (mT)	19	19	19	19	16	19
HF modulation (kHz)	100	100	100	100	100	100
Modulation amplitude (mT)	0.1	0.1	0.1	0.1	0.1	0.1
Number of points	1024	1024	1024	1024	1024	1024
Conversion time (ms)	40	40	20	60	60	20
Time constant (ms)	10	10	10	10	10	10
Sweep time (s)	40.96	40.96	20.48	61.44	61.44	20.48
Number of scans	1	1	1	1-10	1-6 (setup #2a) 1-2 (setup #2b)	4-12

393
394

Figure 1.

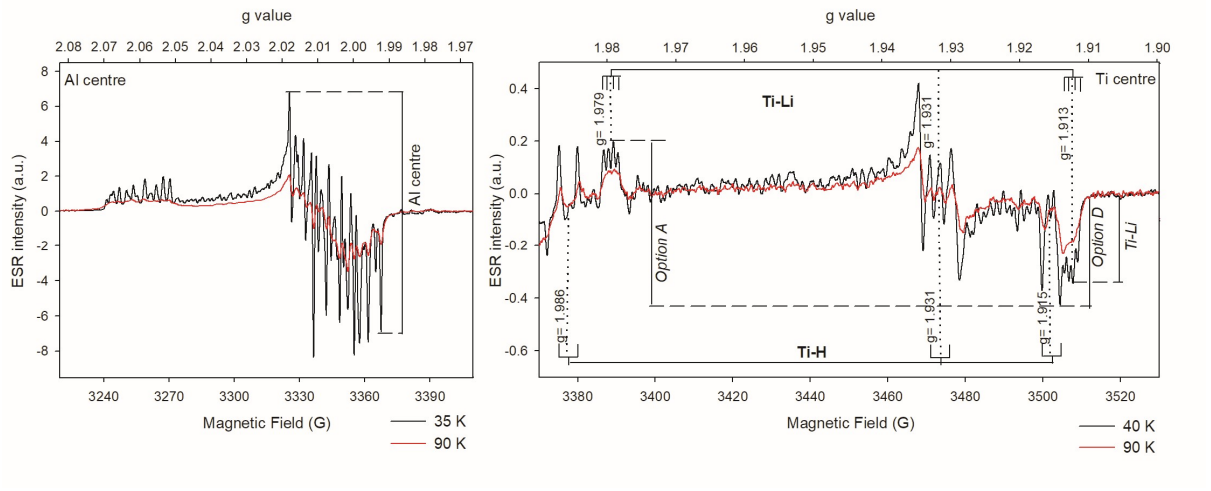
g value
2.08 2.07 2.06 2.05 2.04 2.03 2.02 2.01 2.00 1.99 1.98 1.97
Al centre
ESR intensity (a.u.)
Al centre
3240 3270 3300 3330 3360 3390
Magnetic Field (G)
35 K
90 K
g value
1.98 1.97 1.96 1.95 1.94 1.93 1.92 1.91 1.90
Ti centre
Ti-Li
g= 1.979
g= 1.931
g= 1.913
Option A
Option D
Ti-Li
g= 1.986
g= 1.931
g= 1.915
Ti-H
ESR intensity (a.u.)
3380 3400 3420 3440 3460 3480 3500 3520
Magnetic Field (G)
40 K
90 K

398 **Figure 2.**

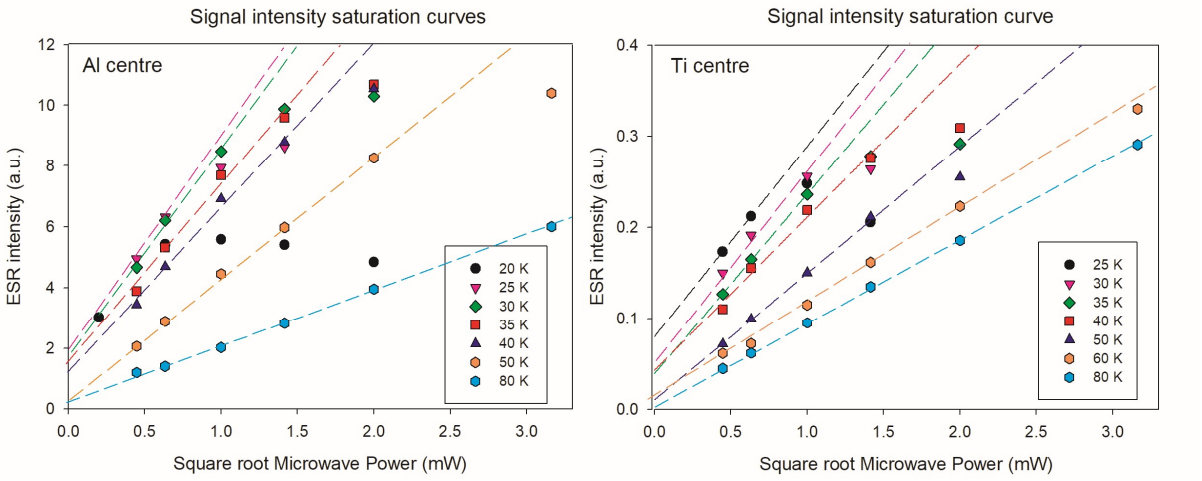

399

400 **Figure 3.**

401

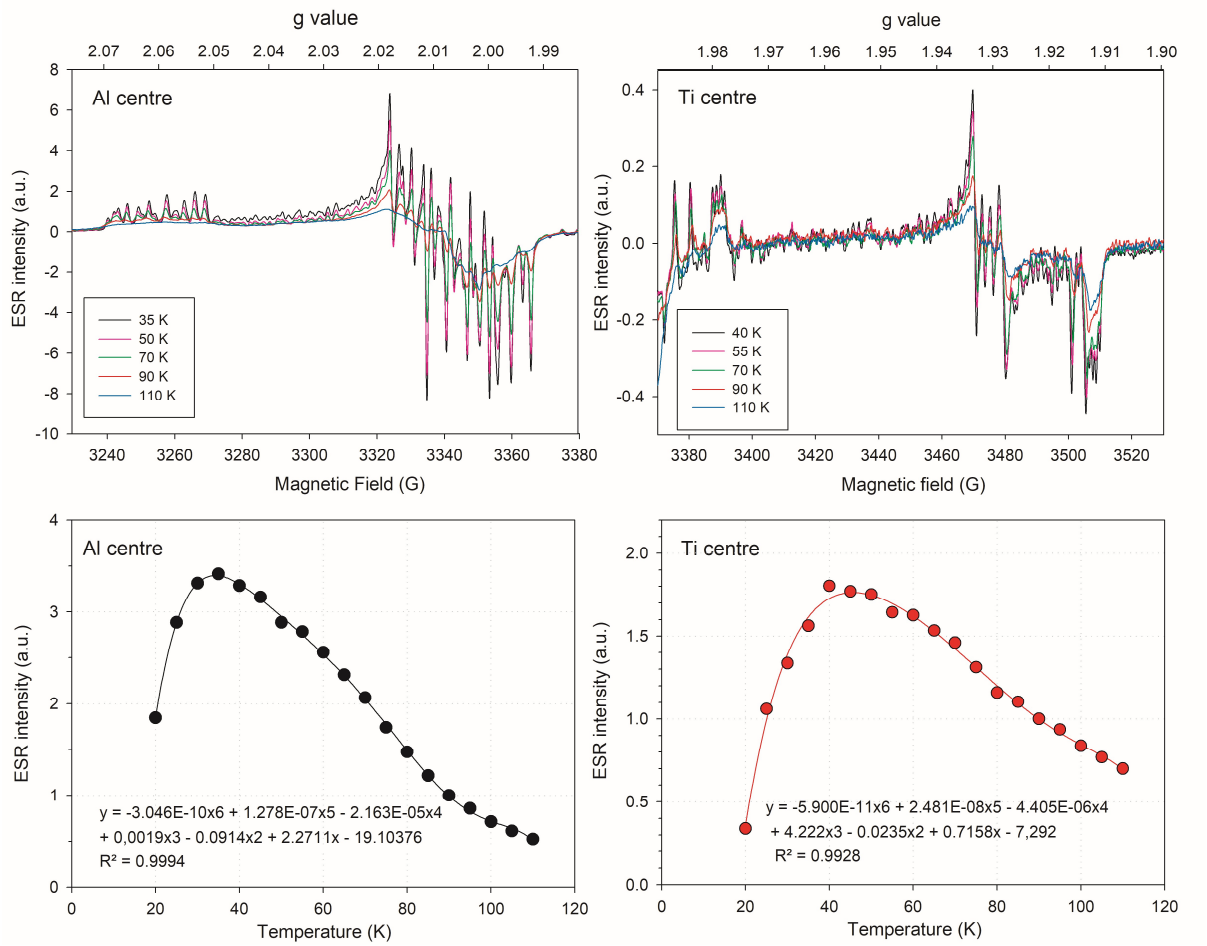

402

403 **Figure 4.**

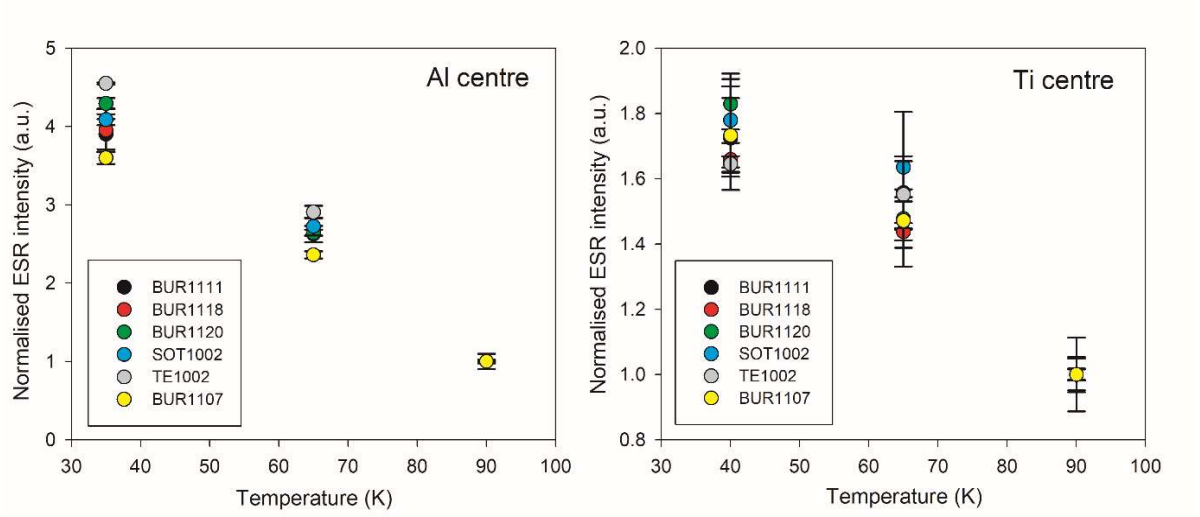

404

405

406 **Figure 5.**

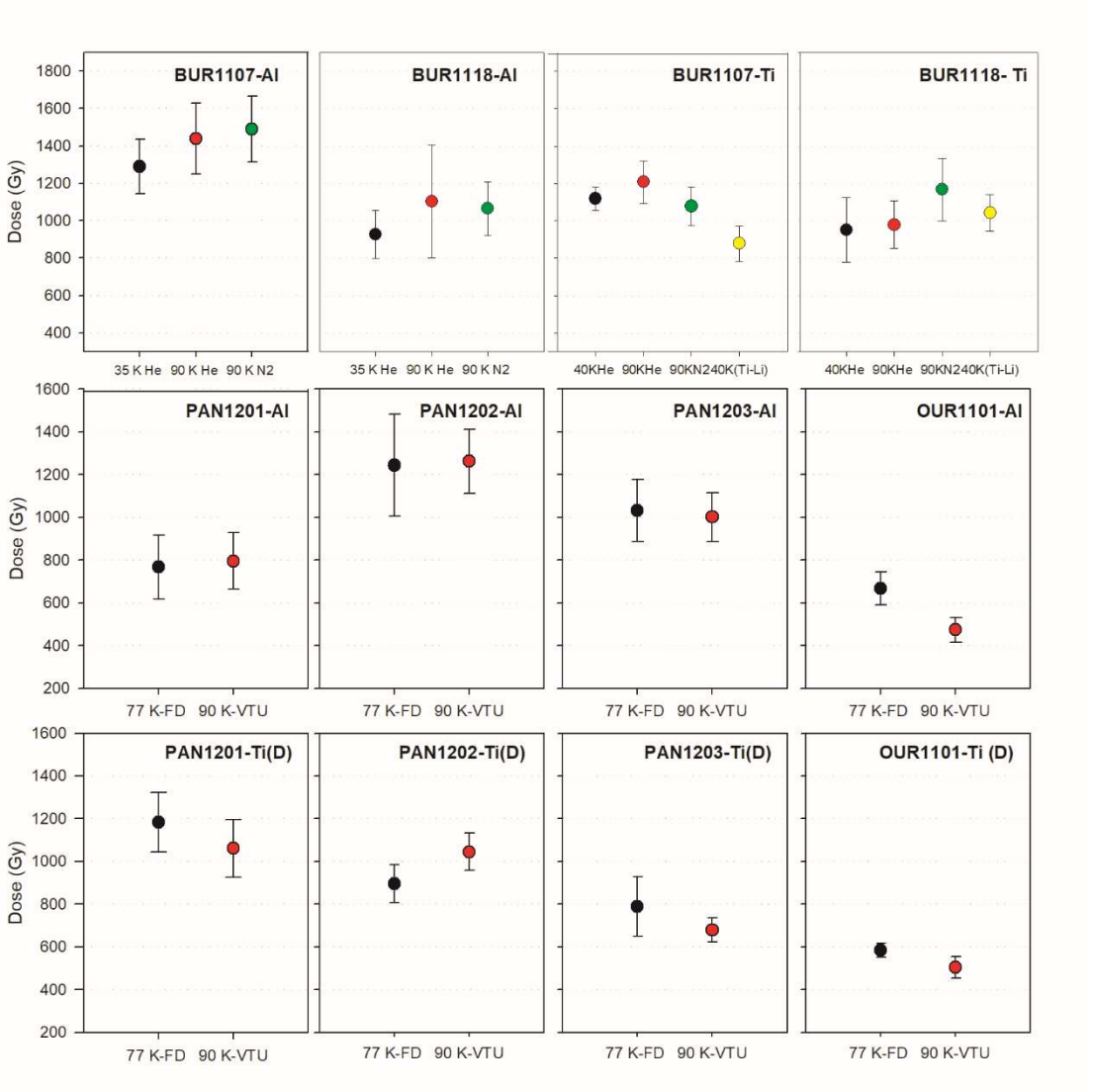

407

408